Distribution of Microstructure and Cooling Rate in Al-Al_2Cu Functionally Graded Materials Fabricated by a Centrifugal Method

Yoshimi WATANABE [a], Yuko HATTORI [a], Hisashi SATO [a, *]

[a] Department of Engineering Physics, Electronics and Mechanics

Graduate School of Engineering, Nagoya Institute of Technology,

Gokiso-cho, Showa-ku, Nagoya, 466-8555, Japan

*Corresponding author

Hisashi Sato

TEL&FAX: +81-52-735-5293

E-Mail: sato.hisashi@nitech.ac.jp

Abstract

Effects of processing parameters, such as type of caster, casting atmosphere and *G* number, on distributions of microstructure and cooling rate in Al-Al_2Cu functionally graded materials (FGMs) by centrifugal casting are investigated. The Al-Al_2Cu FGMs samples fabricated under vacuum have relatively steeper distribution profiles of the Al_2Cu volume fraction rather than samples fabricated under gas atmosphere. Moreover, gradient of the Al_2Cu volume fraction distribution in the FGMs sample becomes larger with increasing *G* number. As well as the Al_2Cu volume fraction, lamella spacing in Al-Al_2Cu eutectic lamella structure is influenced by these processing parameters. These microstructural distributions in the Al-Al_2Cu FGMs samples can be explained by cooling rate distribution in the samples during centrifugal casting. Using the Al-Al_2Cu eutectic lamella structure and the Al_2Cu volume fraction, the cooling rate distributions in the FGMs samples are roughly estimated.

Keywords: Functionally Graded Materials (FGMs); Microstructures; Casting; Cooling Rate

1. Introduction

Functionally graded materials (FGMs) are ones of new composite materials. Miyamoto et al. (1999) have reported that the composition and structure in the FGMs gradually change over volume, resulting in corresponding changes in the properties of the material. As one of the simplest and cost effective techniques for fabricating various FGMs, the centrifugal method, which is application of centrifugal casting, has been proposed by Fukui et al. (1991). In the method, a centrifugal force applied to a homogeneous molten composite assists the formation of the desired gradation. The composition gradient is then achieved primarily by the difference in the centrifugal force produced by the difference in density between the molten metal and solid particles. According to literature by Watanabe et al. (2005), the fabrication of the FGMs containing intermetallic particles made by the centrifugal method can be classified into two categories based on the liquidus temperature of the master alloy. One is a centrifugal solid-particle method, where the processing temperature is lower than the liquidus temperature of the master alloy, and the intermetallic particles in the master alloy are stable in a liquid matrix. As one of investigations concerning with the FGMs fabricated by this method, Watanabe et al. (2001) have investigated about orientation distribution of Al_3Ti platelet particles in the Al-Al_3Ti FGMs three-dimensionally. On the

other hand, if the liquidus temperature is lower than the processing temperature, a centrifugal force can be applied during the solidification both to the nucleated intermetallic particles and to the molten matrix. This method is named as a centrifugal *in-situ* method. By using this method, Watanabe et al. (2005) have investigated about the formation mechanism of gradual microstructure of Al-Al_2Cu FGMs fabricated by the centrifugal *in-situ* method.

Watanabe et al. (1998) have proposed that the velocity of particle motion, *dx*/*dt,* during fabrication of the FGMs by the centrifugal solid-particle method can be determined by the Stokes' law:

$$\frac{dx}{dt} = \frac{|\rho_p - \rho_m| G g {D_p}^2}{18\eta} \qquad (1)$$

where ρ_p, ρ_m, *G, g,* D_p and η are density of particles, density of matrix, *G* number (ratio of centrifugal force to gravity), acceleration due to gravity, particle diameter and apparent viscosity, respectively. In this way, the graded distribution of particle volume fraction in FGMs fabricated by this method is influenced by many processing parameters and materials' constants. As the materials' constants, there are the densities of particles and molten metal. The *G* number and the pipe or ring thickness of products are processing parameters. The particle size and the mean volume fraction of particles are selected to have tailored properties in FGMs. On the other hand, according to

previous study by Watanabe et al. (2007), the viscosity of the molten metal is strongly influenced by the temperature.

In case of the centrifugal *in-situ* method, it was also shown by Watanabe et al. (2004) that the particles size as well as particle volume fraction are distributed in graded manner, and the difference in the particle size distribution within the FGMs is strongly influenced by the difference in cooling process. In addition, Watanabe et al. (2005) have investigated about the formation mechanism of the graded composition in the Al-Al_2Cu FGMs from Al-33mass%Cu eutectic alloy, and they have suggested following mechanism. First, partial separation of Al and Cu elements in the liquid state occurs due to the density difference. A chemical composition gradient is then formed before the crystallization of the primary crystal. The primary crystal in the matrix appears to depend on local chemical composition. Finally, the primary crystal migrates according to density difference, and a further compositional gradient is formed. Since the microstructure is influenced by the cooling process, the formation of graded structure should be not only influenced by materials' constants but also influenced by processing parameters. Therefore, different microstructure may be observed for the FGMs fabricated by the centrifugal *in-situ* method using different centrifugal casters, because the cooling condition of each centrifugal caster is not same.

In this study, the pipe-shaped and the rod-shaped Al-Al_2Cu FGMs are fabricated from Al-33mass%Cu eutectic alloy by using two types of vacuum centrifugal casters. Volume fraction of Al_2Cu and lamellar spacing distributions in the FGMs are evaluated. Basing on obtained results, the cooling rate distributions in the FGMs are roughly estimated.

2. Experimental Procedure

Al-Al_2Cu FGMs are fabricated from Al-33mass%Cu eutectic alloy ingots by two types of centrifugal casters. One is a vacuum centrifugal caster as shown in **Fig. 1**. This caster is designed to be used under both vacuum and desired gas atmosphere, and it has pipe-shape mold. Therefore, pipe-shaped sample is obtained by using this caster. Using this vacuum centrifugal caster, Al-Al_2Cu FGMs samples were fabricated under vacuum condition or N_2 gas atmosphere. The casting conditions by the vacuum centrifugal caster are summarized in Table 1. All of the obtained casts have pipe-shape with 80 mm in outer diameter, 180 mm in length, and roughly 10 mm in wall thickness. After 180 seconds of the casting, the mold pre-heating furnace was turned off and the mold was cooled within the mold pre-heating furnace. Details of the centrifugal *in-situ* method are written in previous papers by Watanabe et al. (2004).

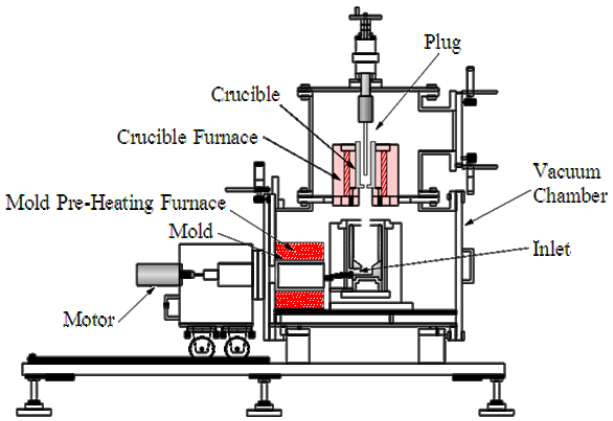

Fig. 1 Schematic illustration of the vacuum centrifugal caster. Shape of casts obtained by this caster is ring or pipe.

Table 1 Fabrication of pipe-shaped FGMs samples by the vacuum centrifugal caster.

Sample	Composition	Pouring temperature	Mold pre-heating temperature	*G* number	Atmosphere
VP1	Al-33mass%Cu	750 °C	500 °C	100	N_2 gas
VP2				1118	
VP3				100	Vacuum
VP4				1118	
VP5			33 °C	1118	

The other caster is a compact vacuum centrifugal caster shown in Fig. 2. This caster has no furnace to pre-heat mold. As mold, the silica molds with two different mold cavities shown in Fig. 3 were prepared. The Al-33mass%Cu alloy was placed in the melting crucible surrounded by the induction coil. The processing temperature was 900 °C or 1000 °C. After the Al-Cu melt reached the desired temperature, the mold and the

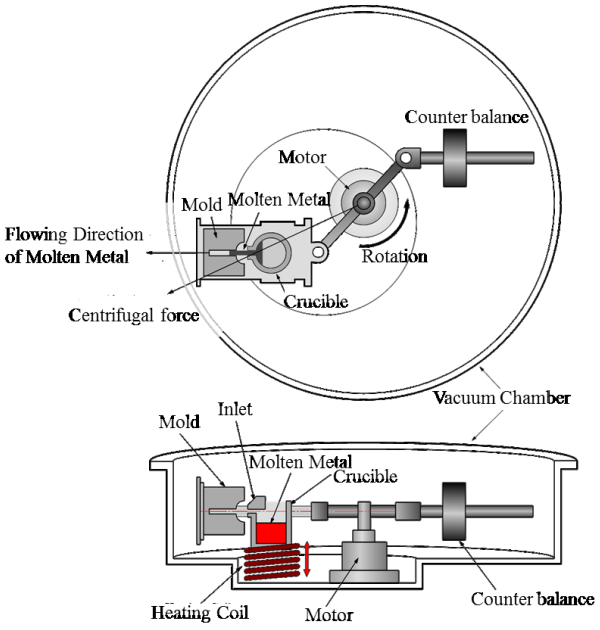

Fig. 2 Schematic illustration of compact vacuum centrifugal caster. Upper and lower illustrations present top and cross-sectional view, respectively. The shape of casts by this machine is rod.

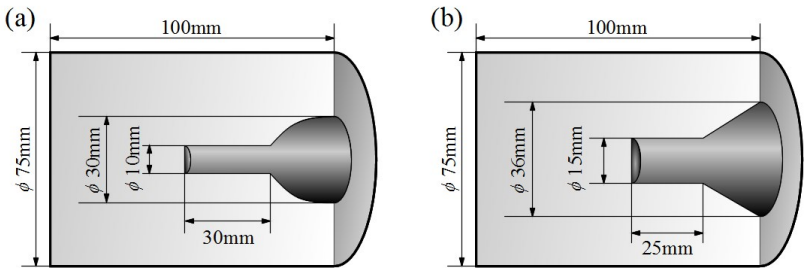

Fig. 3 Cross sectional drawing of the molds for compact vacuum centrifugal caster. (a) mold with 30mm x ϕ 10mm and (b) 25mm x ϕ 15mm.

crucible were rotated for 99 s and the molten Al-Cu alloy was poured into the mold cavity. Shape of the obtained casts is rod-shape. Table 2 shows the details of the fabrication conditions for the rod-shaped FGMs samples.

Each FGMs specimen was divided into ten regions of equal width along the centrifugal force direction for the microstructural observation as a function of position. In case of the rod-shaped FGMs samples, microstructure was observed along center region. The volume fraction of Al_2Cu phase as well as lamellar spacing in each region was measured by optical microscope (OM) or scanning electron microscope (SEM).

Table 2 Fabrication of rod-shaped FGMs samples by the vacuum centrifugal caster.

Sample	Composition	Pouring temperature	Mold temperature	*G* number	Mold diameter	Atmosphere
VR1	Al-33mass%Cu	900 °C	R. T.	78	ϕ 10 mm	Ar gas
VR2					ϕ 15 mm	
VR3				32	ϕ 10 mm	
VR4		1000 °C		78	ϕ 10 mm	
VR5		900 °C			ϕ 10 mm	Vacuum
VR6					ϕ 15 mm	

In order to evaluate cooling rate distribution in the FGMs samples fabricated by centrifugal method, a series of gravity cast experiments was also performed by using Al-Cu alloys with varying cooling rates and copper concentration. Pure Al ingot (99.99 mass%) and Al-40mass%Cu master alloy were used as the elemental materials. Al-20mass%Cu hypoeutectic alloy, Al-33mass%Cu eutectic alloy and Al-40mass%Cu hypereutectic alloy were gravity cast into pre-heating mold with different cooling rates.

The cooling rate was varied by changing the cooling method and mold temperatures. The temperature was measured by thermocouple, and the cooling rate was evaluated as the slope of the cooling curve between 650 ºC and 600 ºC. The casting conditions are given in Table 3. Microstructures of the cast alloys were observed using OM and SEM.

Table 3 Gravity casting conditions.

Composition	Temperature of molten alloy	Cooling method	Mold temperature
Al-20mass%Cu Al-33mass%Cu Al-40mass%Cu	750 ºC	Air cooling	R. T.
			250 ºC
			500 ºC,
		Furnace cooling	N/A

3. Results

3.1 Microstructures of the pipe-shaped samples

Figures 4 (a) to (e) show the typical microstructures of pipe-shaped FGMs samples (specimens VP1 to VP5), respectively. In these figures, left, center and right photographs are taken at inner region, interior region and outer region of the pipe, respectively. The dark and light phases were identified to be Al and Al_2Cu, respectively. The Al and Al_2Cu primary crystals were observed at inner region and outer region of the pipe, respectively. On the other hand, microstructures at interior region of the pipe exhibit an original eutectic structure. Thus, microstructure and local chemical

composition (volume fraction of the Al_2Cu) vary spatially.

Volume fraction of Al_2Cu and lamellar spacing distributions in the pipe-shaped samples as a function of normalized thickness are shown in Figs. 5 (a) and (b), respectively. The normalized thickness means that 0.0 and 1.0 are inner and outer surfaces of the pipe, respectively. The volume fraction of the Al_2Cu was gradually distributed in the pipe-shaped samples, and it increases with increasing the normalized thickness. These results are in agreement with the distribution of the Al_2Cu in the Al-Al_2Cu FGMs reported by Watanabe et al. (2005). Among these FGMs samples, specimen VP5 has most gentle graded profile of the Al_2Cu volume fraction, because of shorter process duration, since the mold was not pre-heated. Comparing between specimens VP1 and VP3 or specimens VP2 and VP4, the specimens fabricated under vacuum have relatively steeper distribution profiles of the Al_2Cu volume fraction. These results may come from difference in cooling rate during the centrifugal casting. It is important to note here that the steeper distribution profiles of the Al_2Cu volume fraction are found in the specimens fabricated under smaller *G* number as comparisons between specimens VP1 and VP2 or specimens VP3 and VP4. Since the microstructure of the FGMs fabricated by the centrifugal *in-situ* method is strongly influenced by the cooling process, the unexpected graded microstructure may be formed. As will be described

later, since evaluation of cooling rate by experimental is very difficult, we will use alternative method to roughly evaluate the cooling rate of the centrifugal casting.

It is also found that the lamellar spacing has position dependency as shown in Fig. 5 (b). Many studies have been made to determine experimentally the dependence of the structure parameter, the lamellar spacing on solidification parameters, *i.e.* temperature gradient, growth rate, and cooling rate. As one of the studies concerning with the dependence of the lamellar spacing on the solidification parameters, Çadirli and Gündüz (2000) have investigated it using lead-tin eutectic alloy. According to the eutectic theory proposed by Jackson and Hunt (1966), Kang and Yoon (2004) have derived the relationship among the growth rate (V), the under cooling (ΔT) and the lamellar spacing (λ) for an isothermal solidification front as

$$\begin{aligned} &\lambda^2 \, \mathrm{V} = B / A \\ &\Delta T / V^{1/2} = 2(A \cdot B)^{1/2} \\ &\Delta T \lambda = 2A \end{aligned} \qquad (2)$$

where A and B are constants. Of course, although the cooling rate was constant during the solidification of eutectic structure, the higher cooling rate results in the larger under cooling. Therefore, the some relation should be existed between the lamellar spacing and the cooling rate.

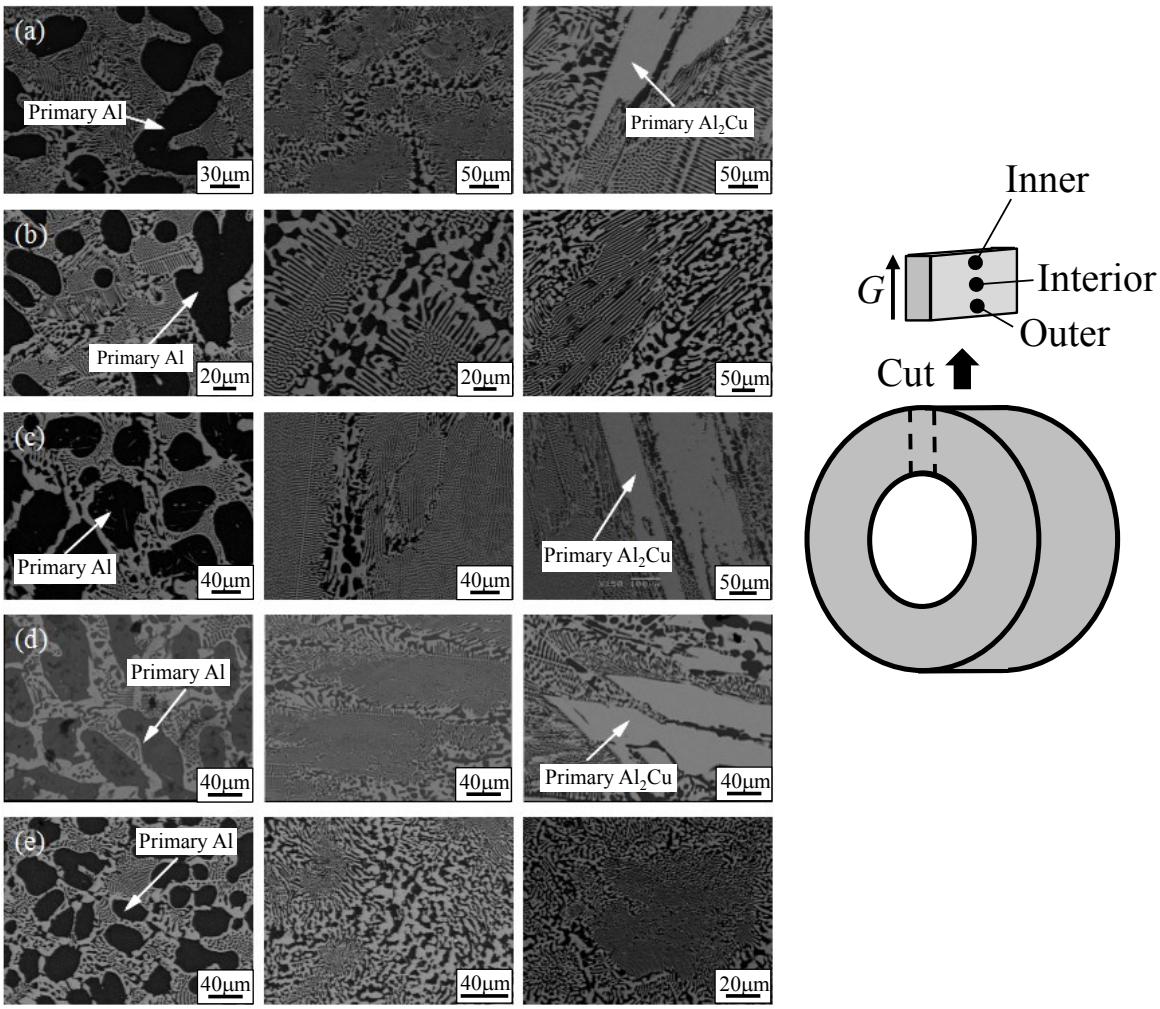

Fig. 4 Typical microstructures of the pipe-shaped samples by the vacuum centrifugal caster at different positions. (a) to (e) are specimens VP1 to VP5, respectively, and left, center and right photographs are taken at pipe inner region, interior region and outer region, respectively. Right-hand side illustration presents observation position.

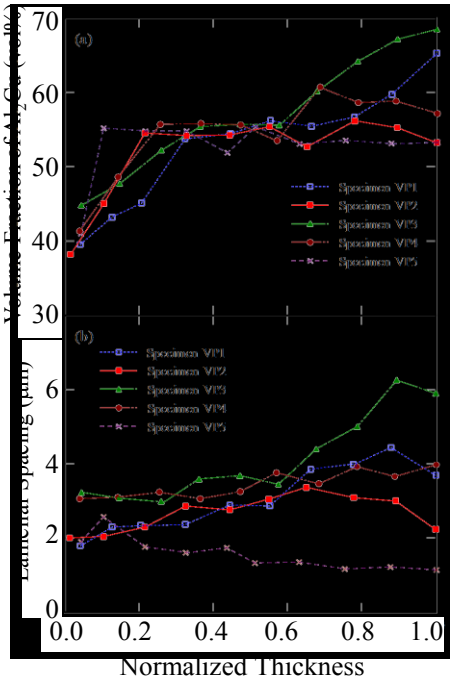

Fig. 5 Volume fraction and lamellar spacing distributions in the pipe-shaped specimens fabricated by the vacuum centrifugal caster.

3.2 Microstructures of the rod-shaped samples

The typical microstructures of rod-shaped samples (specimens VR1 to VR6) at different positions along centrifugal force direction are shown in Figs. 6 (a) to (f), respectively. The left, center and right photographs are taken at inner, middle and outer regions toward the centrifugal direction in the specimens, respectively. Microstructures in rod-shaped FGMs samples are varied spatially. Figures 7 (a) and (b) show the volume fraction of Al_2Cu and the lamellar spacing distributions in the

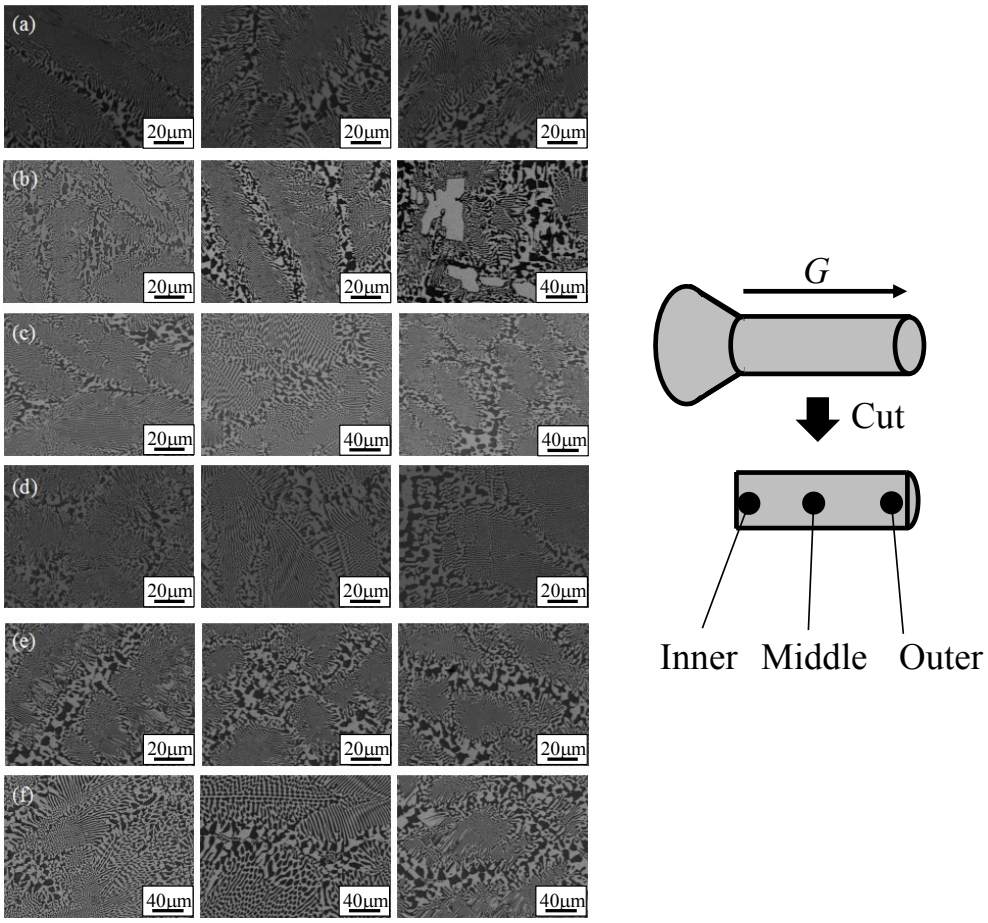

Fig. 6 Microstructures of rod-shaped samples by the compact vacuum centrifugal caster at different positions. (a) to (f) are specimens VR1 to VP6, respectively, and left, center and right photographs are taken at inner, middle and outer regions toward the centrifugal direction in the specimens, respectively. Right-hand side illustration presents observation position.

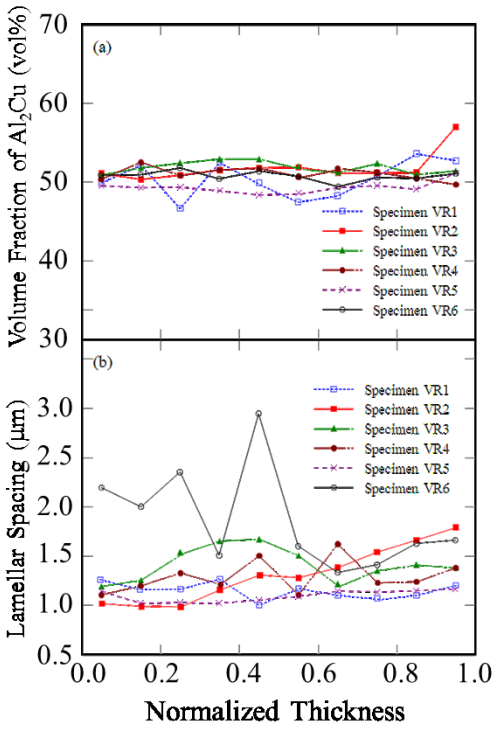

Fig. 7 Volume fraction and lamellar spacing distributions in the rod-shaped specimens.

rod-shaped samples (specimens VR1 to VR6), respectively. As can be seen, smaller compositional gradients are observed comparing with the pipe-shaped samples. This is because the *G* number is smaller and process time of 99 s is shorter. Moreover, smaller lamellar spacing values are found in the rod-shaped samples. This may come from the higher cooling rate, since the mold was not preheated and size of mold is smaller.

4. Discussion

Many simulation studies have been carried out to evaluate the cooling process

of the centrifugal casting and particle segregation during centrifugal method. For example, Ju et al. (1991) have studied the simulation of solidification and temperature in centrifugal casting. However, it has been reported by Kang et al. (1996) that estimation of the temperature distribution during solidification through heat- and mass-transfer analysis under realistic conditions during the centrifugal casting is a complex problem. Experimental studies on cooling process measurements of centrifugal casting were also carried out using thermocouples inserted into the rotating mold. As one of these experimental studies, Murata et al. (1994) have measured the temperature distribution in the rotating mold during the centrifugal casting of Al-Cr alloys. For these studies, special centrifugal caster with a slip ring must be used, where the slip ring is a method of making an electrical connection through a rotating assembly.

Alternatively, in this study, relationship between lamellar spacing and cooling rate was estimated by gravity casting experiment from three Al-Cu alloys with different chemical composition. Using this relationship, the cooling rate distribution inside the Al-Al_2Cu FGMs made by the centrifugal casting will be roughly estimated.

4.1 Microstructures and cooling rate in the Al-Cu alloys by gravity cast

Figure 8 shows the typical microstructures of gravity cast Al-33mass%Cu alloy

samples with different cooling rate. The cooling rates of the samples shown in Figs. 8 (a), (b), (c) and (d) were 12.13 ºC, 6.00 ºC, 2.41 ºC and 0.07 ºC, respectively. It can be noted that the larger lamellar spacing was found for the samples fabricated by slower cooling rate. Similar phenomenon is also observed for the gravity cast Al-20mass%Cu and Al-40mass%Cu alloy samples.

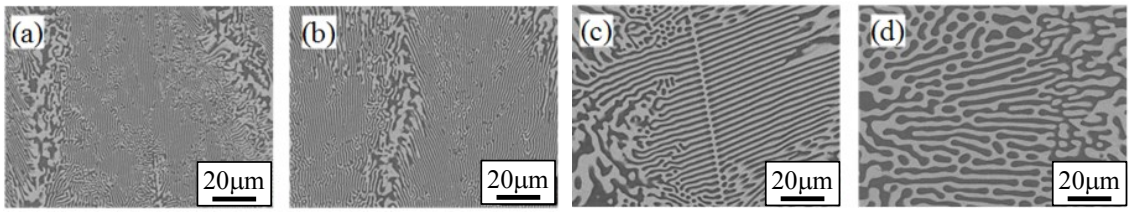

Fig. 8 SEM micrographs of gravity cast Al-33mass%Cu alloy samples with different cooling rate. (a), (b) and (c) samples are air cooled with mold temperature of R. T., 250 ºC and 500 ºC, respectively, while (d) sample is furnace cooled.

Variations of lamellar spacing of the gravity cast Al-20mass%Cu, Al-33mass%Cu and Al-40mass%Cu samples as a function of cooling rate are shown in Fig. 9. The lamellar spacing is strongly influenced by the chemical composition (volume fraction of Al_2Cu) as well as the cooling rate. From Fig. 9, following correlations between the cooling rate and lamellar spacing are determined for each Al-Cu alloy.

$$v = K_1 \exp\left(\frac{3.0920 - \lambda}{0.7657}\right) \quad \text{for Al-20mass\%Cu alloy} \tag{3}$$

$$v = K_2 \exp\left(\frac{3.5138 - \lambda}{0.8768}\right) \quad \text{for Al-33mass\%Cu alloy} \tag{4}$$

$$v = K_3 \exp\left(\frac{1.1492 - \lambda}{4.6834}\right) \quad \text{for Al-40mass\%Cu alloy} \tag{5}$$

where v is the cooling rate in ºC/min, λ is the lamellar spacing in μm and K_1, K_2 and K_3 are coefficients to adjust the dimension of equations.

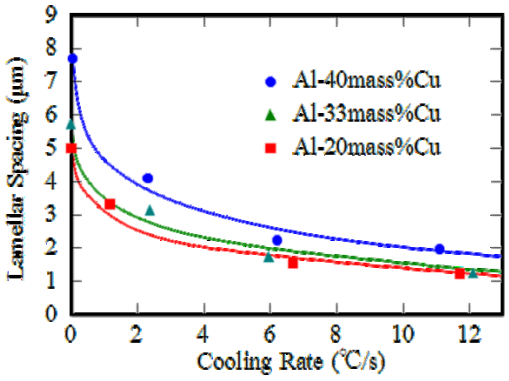

Fig. 9 Relationship between cooling rate and lamellar spacing of gravity cast Al-20mass%Cu, Al-33mass%Cu and Al-40mass%Cu alloy samples.

Volume fractions of Al_2Cu in the Al-20mass%Cu, the Al-33mass%Cu and the Al-40mass%Cu alloys are determined to be 33.6 vol%, 54.5 vol% and 67.5 vol%,

respectively. Then, the effect of volume fraction of Al_2Cu, V_f, on lamellar spacing can be described as

$$\lambda = 0.0015 \times V_f^{\,2} - 0.1086 \times V_f + 4.9601 \qquad (6)$$

when v = 1 °C/min, and

$$\lambda = 0.0007 \times V_f^{\,2} - 0.0545 \times V_f + 2.2941 \qquad (7)$$

when v = 10 °C/min. The equations (3) to (7) allowed us to estimate the quantitative relationship among cooling rate, lamellar spacing and the volume fraction of Al_2Cu.

$$v = K \exp\left\{ \frac{(0.0015 \times V_f^{\,2} - 0.1086 \times V_f + 4.9681) - \lambda}{0.00035 \times V_f^{\,2} - 0.023495 \times V_f + 1.1613} \right\} \qquad (8)$$

In this following, local cooling rate of centrifugal cast will be roughly evaluated from microstructural data and equation (8).

4.2 Cooling rate distributions in the FGMs samples

Fig. 10 shows cooling rate distribution in the pipe-shaped samples roughly estimated from Figs. 5 (a) and (b) and equation (8). Huge position dependence of cooling rate can be observed for specimen VP5, which was fabricated without mold pre-heating, and cooling rate increases with increasing the normalized thickness.

Namely, larger cooling rate is found around pipe outer region, since steel mold was not pre-heated. On the other hand, relatively smaller position dependence of cooling rate was found for specimens VP1 to VP4, which were fabricated with mold pre-heating.

To discuss the effects of atmosphere and *G* number on the cooling rate distribution, Fig. 10 is re-drawn, and results are shown in Fig. 11. Smaller cooling rate is found for the specimens fabricated under vacuum condition (specimens VP3 and VP4) and the cooling rate distribution within the specimen is small, since vacuum is known as a good thermal insulating material. Conversely, the cooling rate of the specimens fabricated under N_2 gas atmosphere (specimens VP1 and VP2) changes from place to place, and larger cooling rate is found around inner and outer regions of the pipe. This is because pipe inner and outer regions make contact with N_2 gas and steel mold, respectively. Comparing the results of specimens VP1 and VP2 fabricated under N_2 gas atmosphere, it is found that the cooling rate around the pipe outer region increases with increasing the *G* number. According to previous study by Watanabe et al. (2004), cooling rate in centrifugal caster without vacuum chamber can be evaluated by using infrared thermometer, and the higher cooling rate was found for lager *G* number case. Present result is in agreement with that previous study, as well as abnormal effects of *G* number on compositional gradients shown in Fig. 5 (a).

Figure 12 shows the cooling rate distributions in rod-shaped specimens (specimens VR1, VR2, VR 5 and VR6) fabricated under centrifugal force of 78*G* at pouring temperature of 900 ºC. Cooling rates are gradually distributed in the larger specimens with ϕ15 mm (specimens VR2 and VR6) while gradients were formed in the smaller specimens with ϕ10 mm (specimens VR1 and VR5), even though the specimen VR1 was fabricated under Ar gas condition. In this way, smaller specimen has a

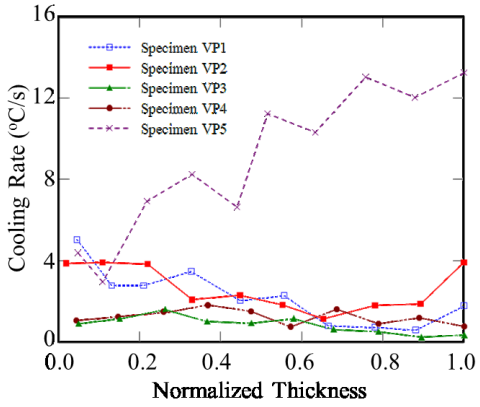

Fig. 10 Cooling rate distribution in the pipe-shaped specimens.

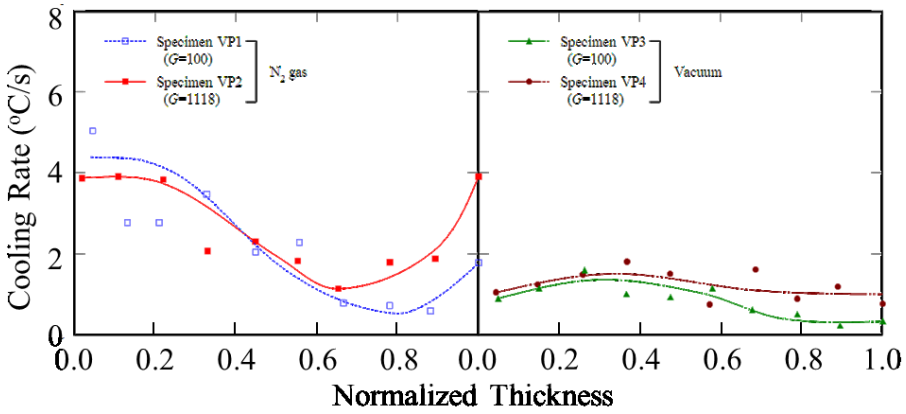

Fig. 11 Cooling rate distributions in the pipe-shaped specimens. These are re-drawn graphs of Fig. 10.

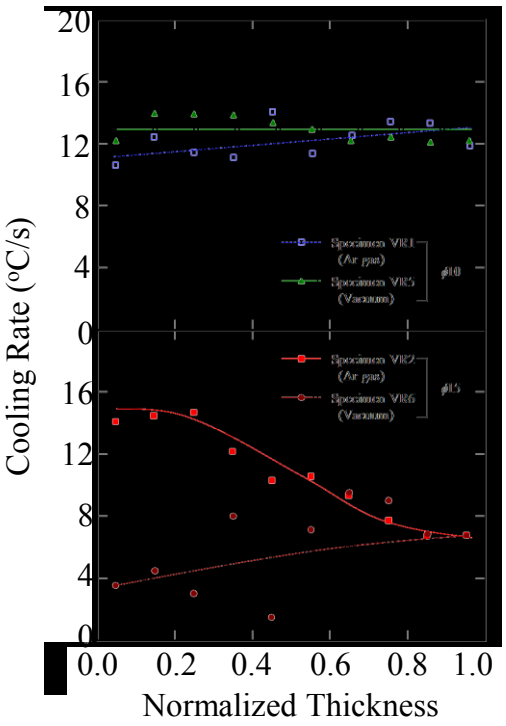

Fig. 12 Cooling rate distributions of rod-shaped specimens under centrifugal force of 78G at pouring temperature of 900 °C. Specimens VR1, VR2 and VR5, VR6 are fabricated under Ar gas atmosphere and vacuum condition, respectively.

tendency to have a homogeneous cooling rate within the cast. Moreover, larger gradient in cooling rate was found for specimen VR2 which was fabricated under Ar gas atmosphere, comparing with specimen VR6 which was fabricated under vacuum condition. Therefore, it is concluded that size of specimen as well as atmosphere influences the cooling rate distribution.

The effects of applied *G* number and pouring temperature on the cooling rate

distribution are shown in Fig. 13. As shown in Fig. 13, lower cooling rate was found

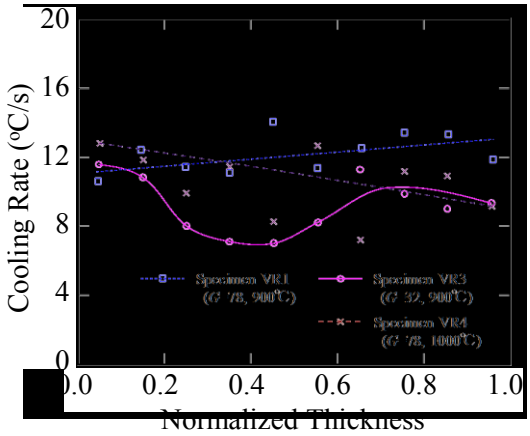

Fig. 13 Cooling rate distributions in the rod-shaped specimens fabricated by different applied G number and pouring temperature.

for the specimen VR4, which was fabricated at higher pouring temperature, comparing with specimen VR1. This is because heat input of specimen VR4 is larger than that of specimen VR1. Moreover, lower cooling rate was found for the specimen VR3, which was fabricated at smaller *G* number. This result is in agreement with the result obtained by vacuum centrifugal system.

4. Conclusions

(1) Distributions of microstructure and composition in the pipe-shaped and rod-shaped Al-Al_2Cu FGMs samples are different depending on position in the samples. These

variations are determined by processing parameters such as cooling rate.

(2) The rod-shaped FGMs samples has smaller compositional gradient comparing with the pipe-shaped FGMs samples. The FGMs samples fabricated under vacuum have relatively steeper distribution profiles of the Al_2Cu volume fraction rather than samples fabricated under gas atmosphere. Moreover, with increasing *G* number, steeper distribution profile of the Al_2Cu volume fraction is formed in the specimen. These can be explained by cooling rate distribution.

(3) Smaller FGMs samples have homogeneous cooling rate distribution rather than larger FGMs samples. Atmosphere and *G* number influence on the cooling rate distribution in the FGMs sample as well as size of sample.

Acknowledgments

This work was supported by “Tokai Region Nanotechnology Manufacturing Cluster in Knowledge Cluster Initiative” by the Ministry of Education, Culture, Sports, Science and Technology of Japan. This study was also supported by “The Light Metal Educational Foundation Inc. of Japan”. These financial supports were gratefully acknowledged.

References

Miyamoto, Y., Kaysser, W. A., Rabin, B. H., Kawasaki, A., Ford, R. G. (Edts.), 1999. Functionally Graded Materials: Design, Processing and Applications, Kluwer Academic Publishers, Boston.

Fukui, Y., 1991. Fundamental investigation of functionally gradient material manufacturing system using centrifugal force. JSME Inst. J. Series III 34(1), 144–148.

Watanabe, Y., Kim, I.-S., Fukui, Y., 2005. Microstructures of functionally graded materials fabricated by centrifugal solid-particle and *in-situ* methods. Met. Mater. Inter. 11(5), 391-399.

Watanabe, Y., Eryu, H., Matsuura, K., 2001. Evaluation of three-dimensional orientation of Al_3Ti platelet in Al based FGMs fabricated by a centrifugal casting technique. Acta Mater. 49(5), 775-783.

Watanabe, Y., Oike, S., 2005. Formation mechanism of graded composition in Al-Al_2Cu functionally graded materials fabricated by a centrifugal in-situ method. Acta Mater. 53(6), 1631-1641.

Watanabe, Y., Yamanaka, N., Fukui, Y., 1998. Control of composition gradient in a metal-ceramic functionally graded material manufactured by the centrifugal method. Composites A 29(5-6), 595–601.

Watanabe, Y., Sato, H., Ogawa, T., Kim, I.-S., 2007. Density and hardness gradients of functionally graded material ring fabricated from Al-3mass %Cu alloy by a centrifugal *in-situ* method. Mater. Trans. 48(11), 2945-2952.

Watanabe, Y., Sato, R., Matsuda, K., Fukui, Y., 2004. Evaluation of particle size and particle shape distributions in Al-Al_3Ni FGMs fabricated by a centrifugal *in-situ* method. Sci. Eng. Comp. Mater. 11(2-3), 185-199.

Çadirli, E., Gündüz, M., 2000. The dependence of lamellar spacing on growth rate and temperature gradient in the lead-tin eutectic alloy. J. Mater. Proc. Tech. 97(1), 74-81.

Jackson, K. A., Hunt, J. D., 1966. Lamellar and rod eutectic growth. Trans. Metall. Soc. A.I.M.E. 236 (8), 1129-1142.

Kang, H., Yoon, W., 2004. Microstructural morphology changes of the lead-tin eutectic alloy by different undercooling levels, Mater. Trans. 45 (10), 2956-2959.

Ju, D.-y., Oshika, Y., Inoue, T., 1991. Simulation of solidification and temperature in centrifugal casting process. J. Soc. Mater. Sci., Jpn 40(449), 144-150.

Kang, C. G., Rohatgi, P. K., 1996. Transient thermal analysis of solidification in a centrifugal casting for composite materials containing particle segregation. Metall. Mater. Trans. B 27B(2), 277–285.

Murata, K., Harada, H., Nakata, T., Umeda, T., 1994. Fabrication of functionally

gradient composite Al-Cr alloys by centrifugal casting. Imono 66(2), 110-115.

Figure Captions

Fig. 1 Schematic illustration of the vacuum centrifugal caster. Shape of casts obtained by this caster is ring or pipe.

Fig. 2 Schematic illustration of compact vacuum centrifugal caster. Upper and lower illustrations present top and cross-sectional view, respectively. The shape of casts by this machine is rod.

Fig. 3 Cross sectional drawing of the molds for compact vacuum centrifugal caster. (a) mold with 30mm x ϕ 10mm and (b) 25mm x ϕ 15mm.

Fig. 4 Typical microstructures of the pipe-shaped samples by the vacuum centrifugal caster at different positions. (a) to (e) are specimens VP1 to VP5, respectively, and left, center and right photographs are taken at pipe inner region, interior region and outer region, respectively. Right-hand side illustration presents observation position.

Fig. 5 Volume fraction and lamellar spacing distributions in the pipe-shaped specimens fabricated by the vacuum centrifugal caster.

Fig. 6 Microstructures of rod-shaped samples by the compact vacuum centrifugal caster at different positions. (a) to (f) are specimens VR1 to VP6, respectively, and left, center and right photographs are taken at inner, middle and outer

regions toward the centrifugal direction in the specimens, respectively. Right-hand side illustration presents observation position.

Fig. 7 Volume fraction and lamellar spacing distributions in the rod-shaped specimens.

Fig. 8 SEM micrographs of gravity cast Al-33mass%Cu alloy samples with different cooling rate. (a), (b) and (c) samples are air cooled with mold temperature of R. T., 250 ^{o}C and 500 ^{o}C, respectively, while (d) sample is furnace cooled.

Fig. 9 Relationship between cooling rate and lamellar spacing of gravity cast Al-20mass%Cu, Al-33mass%Cu and Al-40mass%Cu alloy samples.

Fig. 10 Cooling rate distribution in the pipe-shaped specimens.

Fig. 11 Cooling rate distributions in the pipe-shaped specimens. These are re-drawn graphs of Fig. 10.

Fig. 12 Cooling rate distributions of rod-shaped specimens under centrifugal force of 78G at pouring temperature of 900 ^{o}C. Specimens VR1, VR2 and VR5, VR6 are fabricated under Ar gas atmosphere and vacuum condition, respectively.

Fig. 13 Cooling rate distributions in the rod-shaped specimens fabricated by different applied G number and pouring temperature.

Table Captions